Post-weld heat treatment influence on galvanic corrosion of GTAW of 17-4PH stainless steel in 35%NaCl

Article *in* Corrosion Engineering Science and Technology · June 2011

DOI: 10.1179/174327809X409259

CITATIONS
8

READS
122

3 authors, including:

Mohammad Hadi Moayed
Ferdowsi University Of Mashhad
80 PUBLICATIONS **991** CITATIONS
SEE PROFILE

A. Davoodi
Ferdowsi University Of Mashhad
57 PUBLICATIONS **781** CITATIONS
SEE PROFILE

Post-weld heat treatment influence on galvanic corrosion of GTAW of 17-4PH stainless steel in 3·5%NaCl

M. R. Tavakoli Shoushtari[1,3], M. H. Moayed[1] and A. Davoodi*[2]

The influence of post-weld heat treatment (PWHT), solution annealing followed by aging at 480, 550 and 620°C on the galvanic corrosion in 17-4PH stainless steel weldment in 3·5%NaCl was studied. Potentiodynamic polarisation revealed that all PWHTs improve the passivity of weld region by increasing the pitting potential. Heat affected zone disappears, and base and weld regions act as the anode and the cathode respectively. Zero resistance ammetry measurement for 42 h showed that PWHTs improve the galvanic corrosion resistance by decreasing the galvanic current density to a few to tenths of nanoampere per square centimetre. Aging at 620°C has the highest risk of galvanic corrosion among the three PWHTs. Difference in corrosion characteristic of base and weld were addressed to microstructure variations including ferrite, copper rich precipitates and reverted austenite.

Keywords: 17-4PH stainless steel, PWHT, Galvanic corrosion, Potentiodynamic polarisation, ZRA measurement

Introduction

Alloy 17-4PH (AISI type 630 or UNS S17400) is a martensitic stainless steel containing approximately 3–5 wt-%Cu strengthened by the precipitation of highly dispersed copper particles inside the temper lath martensitic matrix and small fraction of delta ferrite.[1–7] Due to its proper combination of mechanical property and corrosion resistance, application of this alloy has been increased for a variety of usages in marine constructions, chemical industries and power plants.[5,8,9] After solution treatment, 17-4PH exhibits a martensitic microstructure but not enough high hardness. Subsequent precipitation aging treatment in the temperatures between 480 and 620°C results in sub-microscopic, copper-rich phase and increases hardness and strength.[2,4]

Welding processes such as gas tungsten arc welding (GTAW) is frequently used to assemble the 17-4PH components,[10,11] and repair welding is a common technique to reduce the repair and maintenance expenses. However, rapid solidification during welding alters the microstructure and composition in weld zone and also in heat affected zone (HAZ).[10–12] The microstructure of weld spool in 17-4PH mainly contains martensite, but the formation of small fraction of delta ferrite in untempered martensite is also observed.[10] To obtain weldment with approximately similar properties to the base metal, post-weld heat treatment (PWHT) is inevitable. Applying PWHT simultaneously hardens the weld metal, HAZ and base metal and lowers the residual stresses and improves joint efficiencies. Solution treatment of the weld before hardening reduces weld metal ferrite contents and improves its uniformity and strength. However, the toughness of the weld metal decreases with aging temperature above 540°C, probably due to an unfavourable carbide morphology.[10]

The microstructural changes due to welding may also cause electrochemical dissimilarity of individual parts in weldment, which in turn induces galvanic corrosion among base–HAZ, base–weld and HAZ–weld couples exposed to corrosive environments.[10–12] Researches on corrosion behaviour of 17-4PH stainless steel and influence of welding operation and PWHT is scarcely available.[12,13] In the only available paper studying corrosion behaviour of welded 17-4PH stainless steel and effect of PWHT, Nowacki stated that shielded metal arc welding (SMAW) and flux core arc welding (FCAW) provide very good corrosion resistance in 50% HNO_3 solution.[12] Mass loss measurements showed that aging temperature at higher than 620°C ensures better corrosion resistance. However, no electrochemical tests were performed to assess the corrosion behaviour.[12]

On the other hand, since most of reports that has been published on galvanic corrosion are based on measurements between unwelded and welded specimens rather than samples prepared from individual parts of welded specimen, the interpretation of measured current is difficult.[14,15] Recently, galvanic corrosion occurrence of repairing GTAW of 17-4 PH stainless steel in 3·5%NaCl has been studied by the authors.[16] Following this, in the present research, the influence of PWHT on galvanic

[1]Metallurgical and Material Engineering Department, Faculty of Engineering, Ferdowsi University of Mashhad, Mashhad 91775-11, Iran
[2]Materials Engineering Department, Faculty of Engineering, Sabzevar Tarbiat Moallem University, Sabzevar 397, Iran
[3]Materials Engineering Department, Faculty of Engineering, Shahid Chamran University, Ahvaz 61355, Iran

*Corresponding author, email adavoodi@kth.se

Published by Maney on behalf of the Institute
Received 20 August 2008; accepted 10 April 2009
DOI 10.1179/174327809X409259

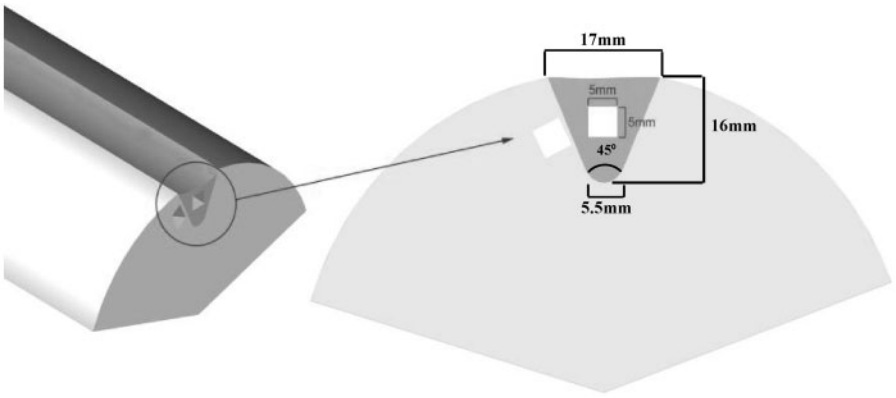

1 Schematic draws of sample extraction from base metal and weld region

corrosion occurrence between base and weld regions in repair welded 17-4PH stainless steel is investigated by utilising microscopic studies, determining the pitting parameters by potentiodynamic polarisation measurements, corrosion potential of three individual zones and passivity current. Individual pieces from base and weld metal was extracted. Moreover, coupled potential and current density was measured by employing zero resistance ammetry (ZRA) technique in 3·5 wt-%NaCl solution, and the results was compared with as welded sample.

Materials and experimental methods

17-4PH stainless steel bar was used with chemical composition of (in wt-%) Fe–0·01C–0·86Mn–0·021P–0·007S–0·8Si–15·74Cr–3·96Ni–0·06Mo–2·74Cu–0·3(Nb + V), which is in agreement with the ASTM A705 (grade 630) standard for precipitation hardening forged stainless steel.[17] The as received samples delivery condition is shown in Table 1 (label I). A repair welding procedure was performed to simulate the existence of piratical metallurgical defects, as shown in Fig. 1. Gas tungsten arc welding operation using ER630 filler electrode (with chemical composition of Fe–0·032C–0·54Mn–0·021P–0·01S–0·37Si–16·2Cr–4·59Ni–0·68Mo–3·9Cu–0·27(Nb + V) was performed. The welding parameters were as follows: current, 130–150 A; voltage, 14–16 V; welding speed, 180–200 mm min^{-1}. Argon with purity of 99·999% with 11–14 L min^{-1} flowrate has been used as protective gas. After welding operation, three different PWHTs, labelled II, III and IV, based on ASTM A705,[17] were performed, as summarised in Table 1, to obtain peak-aged, intermediate and overaged specimens.[18] Metallographic samples were then extracted from weldment, grinded from 60 to 1200 SiC papers before finishing by 1 μm diamond paste. To determine the weld area and HAZ zone, the sample was exposed to a Marble's reagent (4 g $CuSO_4$, 20 mL HCl and 20 mL distilled water) for macroetch examination. To identify the microstructure constituents in weldment, Vilella's reagent (1 g picric acid, 100 mL ethyl alcohol and 5 mL hydrochloric acid) was used. Scanning electron micrographs of base alloy and weld region were taken by Leo1455VP SEM instrument with 1500 kV power. Hardness test, Rockwell C, was performed using Avery–Denison instrument in three regions, 3 points in each area. For corrosion studies, identical samples of base and weld regions were obtained, as shown schematically in Fig. 1, with cross-section area of 5 × 5 mm for weld and base regions (note that HAZ disappeared as a result of PWHT, see the section on 'Microstructure evaluation'). Before corrosion tests, the samples degreased in 10%NaOH for 1 min at 50–60°C, washed by distilled water, ultrasonically cleaned in acetone for 2 min in room temperature and dried. To avoid the crevice corrosion during the corrosion tests, the interface between sample and mounting material was covered by lacquer.[14]

Table 1 Summary of PWHT on 17-4PH used in this research

Label	Conditions	Heat treatment
I	As received	Condition A (1 h)→oil quench→ 550°C (4 h)→air cool→ 620°C (4 h)→air cool
II	H900	Condition A (1 h)→480°C/1 h→air cool
III	H1025	Condition A (1 h)→550°C/4 h→air cool
IV	H1150	Condition A (1 h)→620°C/4 h→air cool

An ACM potentiostate (ACM Instruments) was employed for the electrochemical tests, including the specimen as working electrode, saturated calomel as reference electrode and platinum wire with surface of 2 cm^2 as counter electrode. All corrosion tests were performed in a 3·5 wt-%NaCl solution at ambient temperature. To obtain pitting parameters, potentiodynamic polarisation measurement was carried out with a slow scan rate of 3 mV min^{-1} in a range of 200 mV cathodic potential up to the anodic breakdown potential. Each test was repeated three times to ensure reproducibility, and the average values were reported. Moreover, passivity behaviour was evaluated by potentiostatic polarisation of individual base and weld zones at an anodic potential of 200 mV. The aim was to examine resistance to pitting corrosion in samples within the passivity zone. Before potentiostatic polarisation, each sample was first placed for 60 min in the solution to stabilise the potential. Finally, coupled potential and current density of the possible galvanic cells in PWHT samples between the weld and base regions were measured by ZRA during 1 and 42 h. For 42 h measurement, the data points for 10 min have been collected every 6 h.

Results and discussion

Microstructure evaluation

First stage in PWHT is the solution annealing, which removes detrimental effects of HAZ compare to the as weld specimen.[16] As seen in Fig. 2, comparing

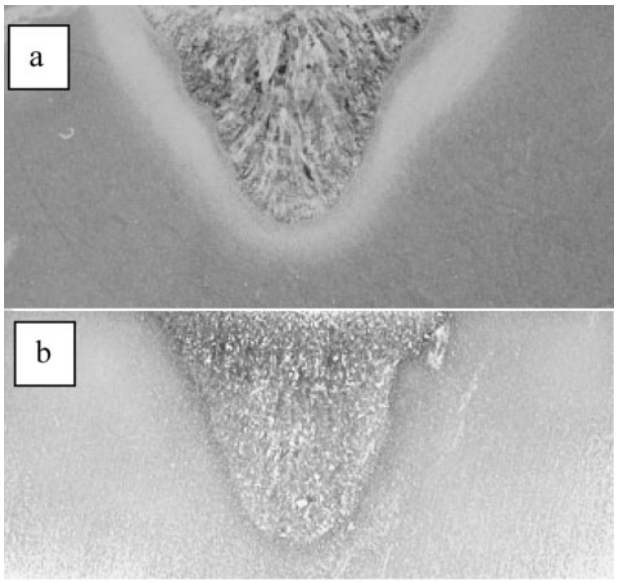

2 Macrography examination of weldment of *a* I and *b* IV showing that HAZ disappeared

macroetch examination of weldments in I and IV (as an example) reveals that that solution annealing leads to vanishing of the HAZ. Only fusion line appears between base and weld region. By removing the HAZ, therefore, in this study, all measurements and characterisations are represented for base and weld regions. The microstructure of 17-4PH samples in base and weld regions, in conditions II, III and IV are shown in Fig. 3 (the microstructure of as received sample, label I, was described in more details previously).[5,16] Although microstructure varies by increasing the aging temperature, all PWHTs improve more or less microstructure similarity in base and weld regions compared to as weld weldment.[16] In addition, it is clear that the volume fraction and the morphology of surface constituents have been changed. However, optical microscopy is clearly sufficient to reveal the details of the martensite matrix. Figures 4 and 5 depict the SEM images of microstructure in the base region in samples II, III and base and weld zone in sample IV. In II, tempered lath martensite formed on prior austenite grains has been detected. On the contrary, III and IV depict a microstructure similar to the Windmännstätten structure, different from typical tempered martensite structure. They consist of recrystallised ferrite phase (appeared as white lamellar layer in Figs. 4 and 5) formed in the tempered martensite. More details of this structure can be seen in Fig. 4*c*. Image analysis revealed that, by increasing the aging temperature from 550 up to 620°C, the amount of lamellar layers has been increased up to 42% in volume fraction. On the contrary, no lamellar white structure was observed in II (Fig. 4*a*). It has been reported that such lamellar structure is present in a microstructure of 17-4 PH alloy aged at temperatures above 570°C, which may be related either to the formation of reverted austenite or recrystallised alpha ferrite in the tempered martensite. Based on the size and quantity of this lamellar structure in the present study, the second postulate is more reliable.[5] Figure 5*b* shows the microstructure of weld region of GTA welded 17-4PH in IV. The results reveal that utilising PWHT, including solution annealing followed by age hardening, leads to the reduction in the dissimilarity of weld and base region, which is in agreement with the literature. Similarity of weld and base zones in specimens II and III has also been found, as shown in Fig. 3. This can be confirmed by hardness measurement on base and weld regions on samples I, II, III and IV, as presented in Fig. 6. The profile shows that performing all PWHTs contributed to the more even hardness distribution. Sample I has the most uneven hardness distribution; while the hardness in the base region is about 38 HRC, it decreases down to 30 HRC in HAZ and increases again in weld region up to 32·5 HRC. On the other hand, by increasing the aging temperature from 480 up to 620°C, hardness value decreases from 43·5 to 30 HRC. Although the lowest aging temperature, 480°C, results in considerably higher hardness value, it is also results in embrittlement of the microstructure, which is not favourable.[3] In this temperature, the copper precipitates are still coherent and do not cause large strain contrast due to the small strain field around the precipitates,[2] and therefore, this fine coherent Cu-rich clusters in matrix is be found to enhance hardness significantly.[7,18] Excessively high aging temperature has reverse influence and significantly softens the structure, as can be seen in the hardness values in Fig. 6 at 620°C. This can be attributed to the coarsening of the incoherent ε-Cu rich precipitates and formation of slight amount of reverted austenite and partially lamellar ferrite phase.[5,18,19] Applying an aging procedure at 550°C produces an even hardness distribution around 37 HRC. Therefore, considering the hardness measurement, intermediate temperature around 550°C is the optimal condition.

In summary, PWHTs reduce the non-uniformity of microstructure and hardness between weld and base regions in GTA welded 17-4PH stainless steel. The influence of PWHTs on corrosion behaviour of weldment is shown in the following sections. It should be mentioned that the results of corrosion studies on individual parts of as weld specimen have been previously reported elsewhere.[16]

Potentiodynamic and potentiostatic measurements

The slow scan rate potentiodynamic polarisation curves of individual base alloy and weld zone of 17-4PH stainless steel for II, III and IV are shown in Fig. 7. The values of OCP (after 1 h immersion time), the pitting potential E_{pit} and passivity current i_{pass} were obtained, and the results are shown in Table 2 (the data of as weld specimen was borrowed from a previous study by the authors).[16] Generally, all aging heat treatments improve, in various extensions, both rest potential and pitting parameters. Moreover, PWHTs also reduce both OCP and pitting potential difference between the base and weld regions. Based on the OCP values, in all conditions II, III and IV, the base and the weld regions act as an anode and cathode respectively. The OCP difference between base and weld regions in III has the highest value, which is about 20 mV, while after 1 h exposure time, this value, in the case of II, is about 8 mV. This means that considering OCP difference as a thermodynamically driving force of galvanic corrosion, it can be predicted that, during 1 h exposure time, galvanic current in base–weld couple in III is the highest value

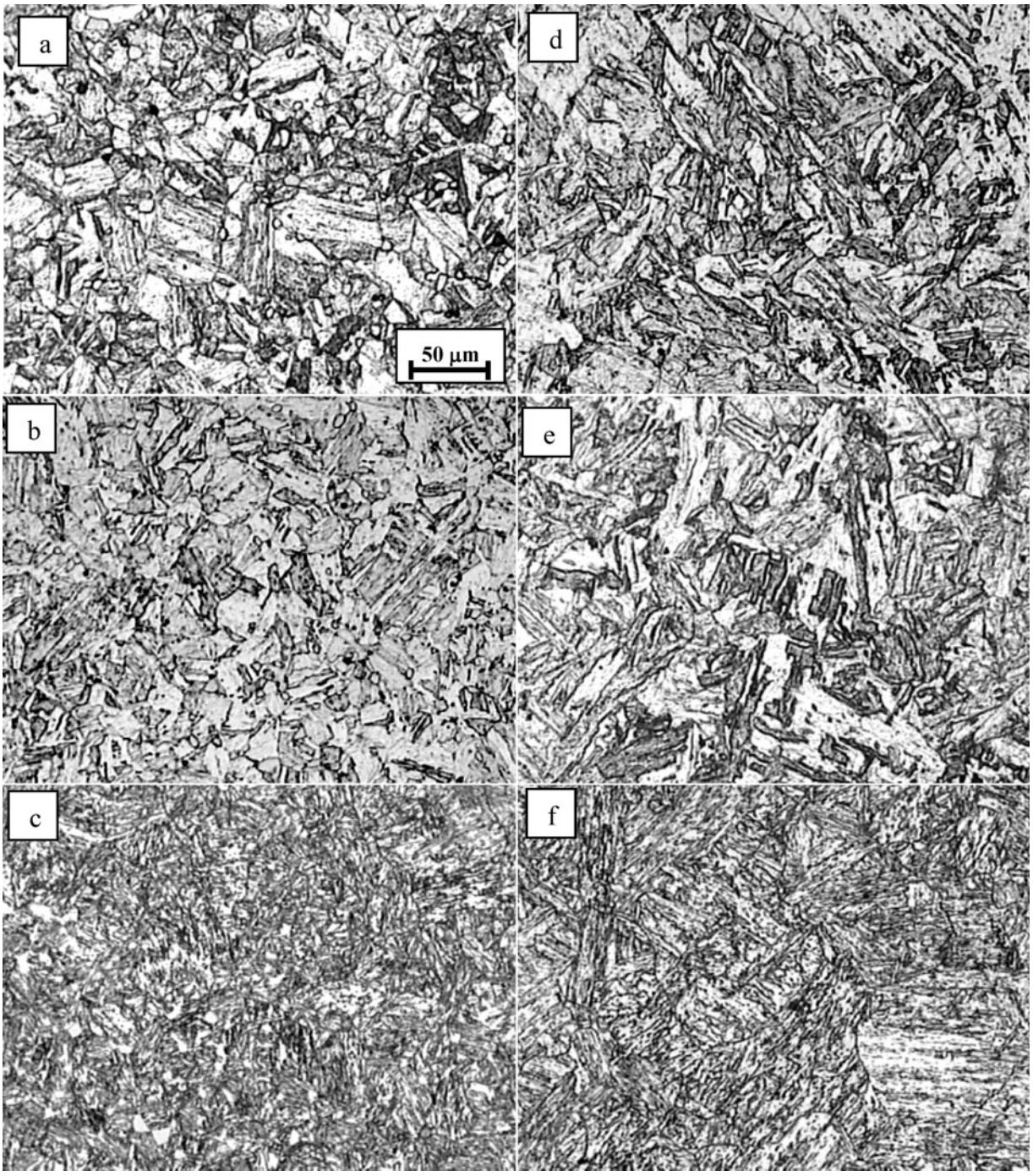

3 Optical images of *a–c* base and *d–f* weld regions of GTA welded 17-4PH in three different PWHT conditions (II, III and IV) respectively

compared with the base–weld couples in II and IV (*see* Table 2). However, PWHTs significantly reduce the OCP difference between galvanic couples compared with as weld from 55 mV to the minimum 8 mV in specimen II, due to the elimination of the microstructure dissimilarity of two regions, as shown in Fig. 3. In addition, while aging heat treatment in 480 and 550°C slightly increases, the OCP of base region from −130 to −118 and −120 mV respectively compared with the base region in as weld specimen;[16] in 620°C, the OCP remains unchanged. In contrast, comparing OCP values in weld regions reveals that, while aging at 550°C modifies the OCP from −110 to −100 mV, it reduces the OCP to −118 mV by aging at 620°C, remaining unchanged after aging at 480°C (*see* Table 2). There had been limited data available for statistical evaluation of OCP, with only three times repetition. However, they replicated each other, and it seems that, although the potential differences of a few millivolts between base and weld regions seems to be too low, it can be seen later, during galvanic connection between them, that these small differences could generate galvanic current in the range of nanoampere, which is detectable with low noise potentiostat instrument with faraday's cage. Therefore, these differences were meaningful, and main efforts have been made to detect the galvanic current.

Concerning to the pitting resistance, it appears that, by increasing aging temperature from 480 to 550°C, the

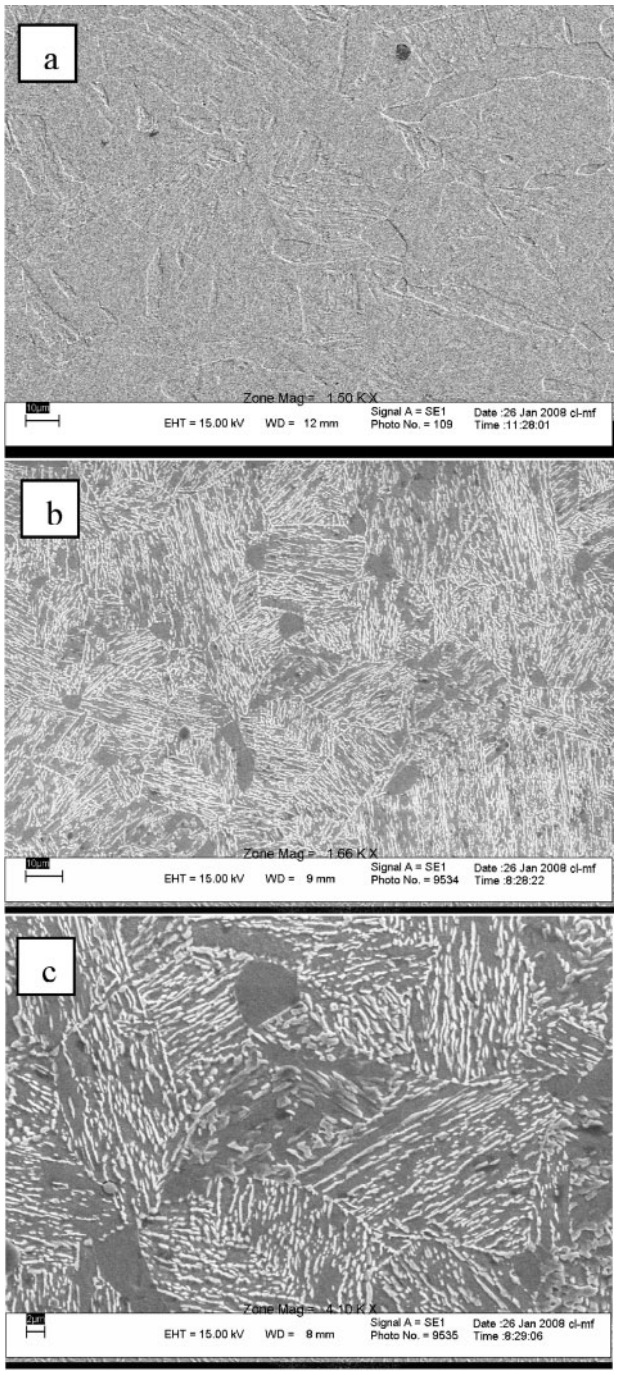

4 Images (SEM) of *a* II, *b* and *c* III of base region of GTA welded 17-4PH

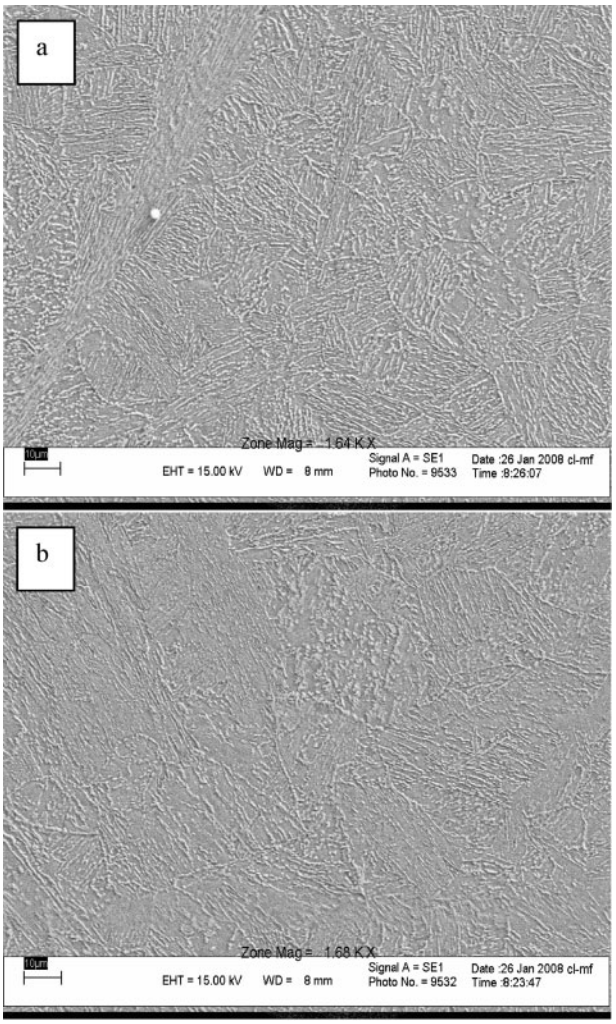

5 Images (SEM) of *a* base and *b* weld regions of GTA welded 17-4PH in IV respectively

pitting potential in base and weld regions is significantly raised, but further increasing the aging temperature up to 620°C reduces the pitting potential down to +124 and +133 mV in base and weld zones respectively (Table 2). Therefore, aging at 550°C results in the highest pitting resistance both in base and weld zones. Comparing as weld and PWHTs samples also indicate an improvement in pitting resistance due to aging heat treatment, which is more enhanced in III. Three times repetition of experiments also confirmed that the pitting potential differences are meaningful.

The passivity currents in the range of 0·1 to 0·3 $\mu A\ cm^{-2}$ is obtained for PWHT samples, which are almost similar to the as weld specimen. In II, the passivity current in base metal is almost twice than the weld region. On the contrary, in III and IV, the passivity current in weld zone is reversely more than the base region, as shown in Fig. 7.

By utilising a very slow scan rate (3 $mV\ min^{-1}$) potentiodynamic polarisation, the existence of metastable pits could be also exhibited as the current fluctuations in passivity range (Fig. 7). In passivity potential domain, the amplitude of fluctuations is bigger

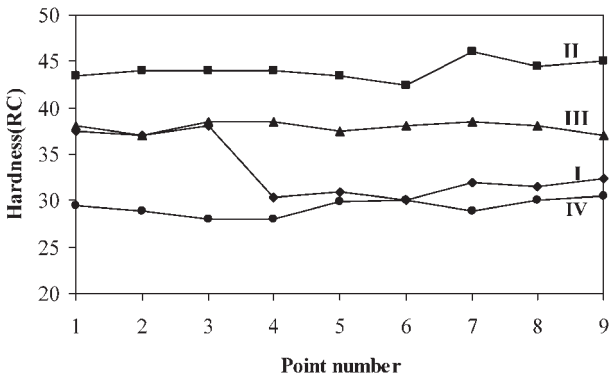

6 Hardness profile measure along base, HAZ and weld regions in repair welded 17-4PH stainless steel in I, II, III and IV

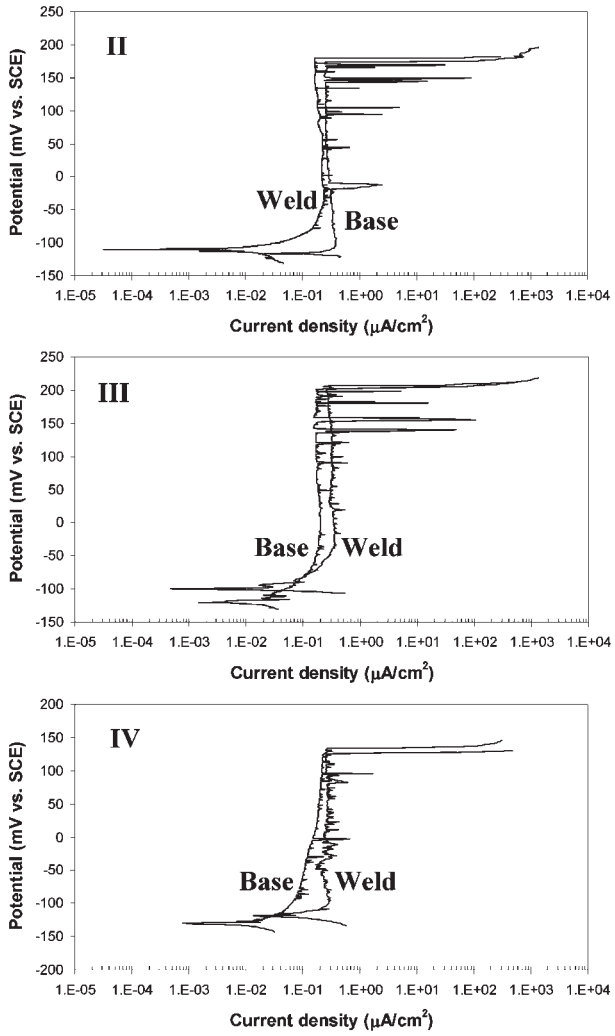

7 Potentiodynamic polarisation curve for individual base and weld regions of repair welded 17-4PH stainless steel in II, III and IV, immersed in 3·5%NaCl solution. Scan rate was 3 mV min^{-}

in II and III than the one in IV, while the fluctuation frequency (the number of current peaks) is greater in IV than in II and III. This means that the pitting sites in IV are much more than that in II and III, but they generate less current compared with II and III. The difference in amplitude and frequency of metastable pits can be attributed to the microstructure changes,[20] (as described in the section on 'Microstructure evaluation') including the volume fraction and the morphology of constituents and precipitates during various aging heat treatments.

Table 2 Values of OCP (after 1 h immersion time), pitting potential E_{pit} and passivity current i_{pass} in I, II, III and IV

Condition	Region	OCP, mV	E_{pit}, mV	i_{pass}, μA
I	Base	−130	+50	0·13
	HAZ	−165	−7	0·2
	Weld	−110	+130	0·13
II	Base	−118	+173	0·27
	Weld	−110	+180	0·16
III	Base	−120	+205	0·18
	Weld	−100	+201	0·32
IV	Base	−130	+124	0·1–0·22
	Weld	−118	+133	0·27

In summary, potentiodynamic polarisation measurements reveal that in III, PWHT at 550°C, leads to the optimum corrosion resistance including higher OCP, pitting potential and passivity potential domain. Conversely, aging at 620°C, results in the worst corrosion resistance.

Figure 8 shows the passive current density variations through 900 s exposure time for weld and base zones of 17-4PH stainless steel by applying constant anodic potential of 200 mV with respect to the rest potential in a 3·5 wt-%NaCl solution. Applying 200 mV anodic potential versus OCP of each area leads to more or less similar conditions, and OCP of each area has been chosen as reference point because they were more convenient. Similar trend of results are expected to be obtained if the applied potential in the passivity changes slightly (around tenth of microvolt). Therefore, the general conclusion does not change significantly. Using 900 s as a period for potentiostatic test is based on the fact that, after 900 s, it can be seen that the trend of current density has reached a steady state. This is a sufficient time to evaluate the passivity current density, i.e. tests do not need to be continued further. It can be observed that further time does not change meaningfully the values that have been reported by authors as passivity current density in potentiostatic tests. Therefore, by applying the 200 mV anodic potential, all specimens has reached the passivity state. The passivity current densities in base and weld zones decreased with time, and the passivity current densities decreased faster in base metals in all conditions. Apparently, the passivity integrity in base zone in III and IV is better than that in the weld zone, while aging at 480°C in label II results in higher passivity current (*see* Fig. 8). After 900 s, the steady state passive current of base region reaches 1·15, 0·09 and 0·06 μA cm^{-2} in II, III and IV respectively. In weld region, the corresponding values are 0·6, 0·56 and 0·41 μA cm^{-2} for II, III and IV respectively. Comparing potentiostatic results of PWHT samples to as weld specimen[16] indicates that heat treatment does not have a significantly influence on passivity current of weld region. However, aging at 550 and 620°C decreases the passivity current in base metal with respect to as weld, which is a benefit. The irregular current fluctuations observed on potentiostatic measurement can be attributed to the formation of metastable pits, which is more enhanced in welds of II and IV. Interestingly, no current fluctuations are seen in the weld of III. This again confirms the previous potentiodynamic measurements in Fig. 7. In comparison, the base region of sample II shows the highest current fluctuations up to 4 μA cm^{-2} among three samples.

Zero resistance ammetry measurements

Based on corrosion potential difference between base and weld regions from potentiodynamic polarisation curve (Fig. 7), in all cells, the base and weld regions act as anode and cathode respectively. The galvanic current densities were measured by ZRA method for the galvanic couples of base–weld of 17-4PH in II, III and IV for 1 and 42 h exposure time. The result of galvanic current density and couple potential for 1 h experiment is presented in Fig. 9. Generally, the galvanic current density of IV couple is significantly higher than two others, with the average around 100 nA cm^{-2} and

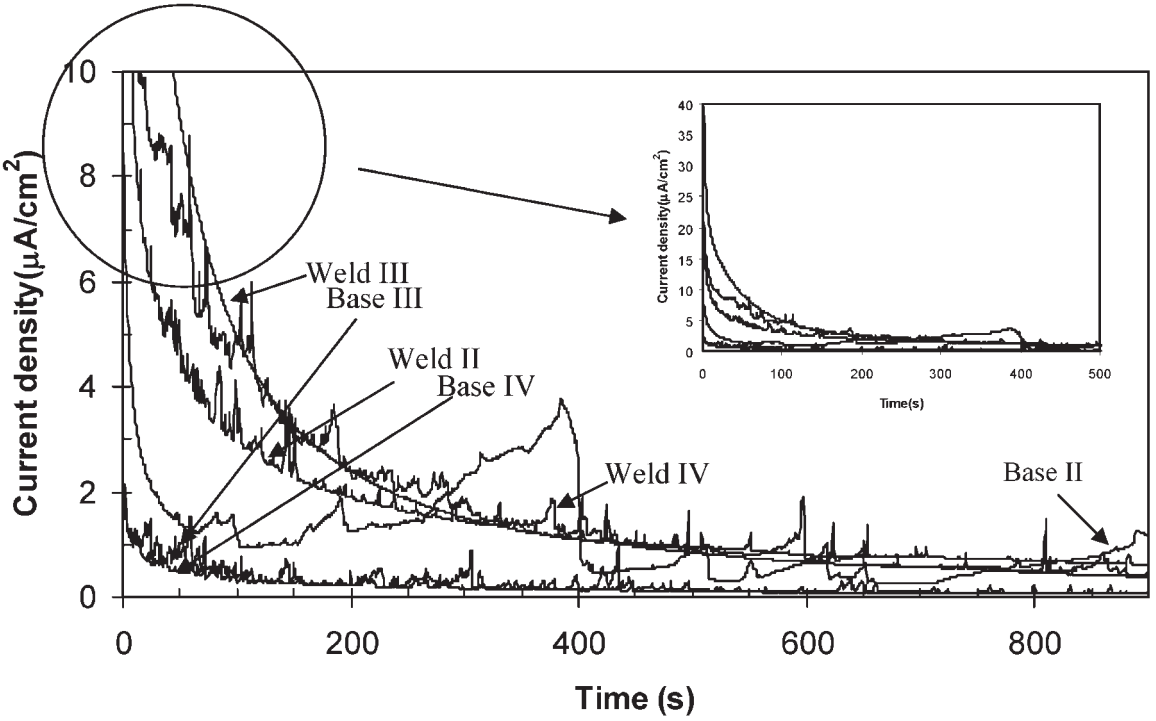

8 Potentiostatic curve for individual base and weld regions of repair welded 17-4PH stainless steel in II, III and IV in 3·5%NaCl solution during 900 s. Anodic potential was 200 mV offset to rest potential

shows much greater current fluctuations up to 200 nA cm^{-2} during 1 h exposure time. Considerably lower galvanic current was monitored in II and III, which reached the current level of about 18 nA cm^{-2}. Taking into account the results of as weld specimen,[16] PWHTs reduced galvanic couple current between base and weld regions, which is more enhanced in II and III. Heat affected zone disappears by applying PWHT, and the most dangerous couple, weld–HAZ, with 400 nA cm^{-2} galvanic current, was also removed. Couple potential variations of the cells presented in Fig. 9*b* reveals a gradual increase in potential, which can be attributed to the equal positive shift of anode and cathode OCPs (since the couple current is almost constant), and indicate the consistency and continuity of passivity on both electrodes, similar to as weld specimen.[16]

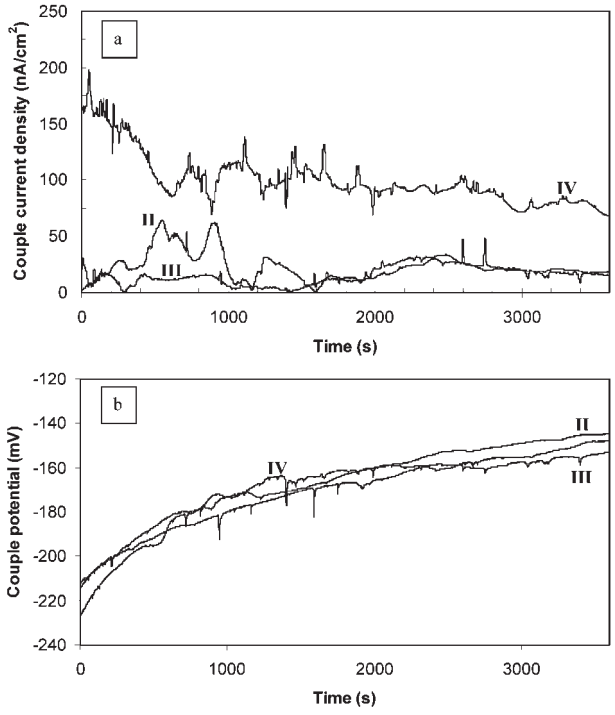

9 *a* galvanic couple current density and *b* couple potential of weld–base in II, III and IV during 1 h exposure time in 3·5%NaCl solution measured by ZRA method

In summary, PWHT improves galvanic corrosion resistance and reduce remarkably the current density in base–weld pairs in II and III and with less extension in IV. However, caution should be taken into account to judge the galvanic corrosion based on 1 h measurement, and longer exposure time measurement is needed. To better evaluate galvanic corrosion occurrence, longer test has been carried out by ZRA measuring for 42 h. For every 6 h intervals, 600 s data points were collected, and the results of seven measurements for 42 h were presented in one graph as described previously.[16] These data were collected for all three couples of weld–base in II, III and IV. To simplify the interpretation, the average values of each 600 s data point collected for 6 h intervals are shown in Fig. 10. The data for flushing time, the initial instant time less than 6 h, have not been shown in the graph. Again, remarkably lower current densities are observed for II and III. Couple galvanic current between base and weld in II and III gradually decrease and reach to almost steady state around 2 and 6 nA cm^{-2} respectively. It can be predicted that after 42 h exposure time, current density decreases gradually (Fig. 10*a*). An increase in couple potential and simultaneously a decrease in galvanic current density may be an indication of passivity improvement as a result of passive film modification and thickening. On the contrary, the galvanic current in IV (which is even lower than sample III in the beginning) decreases until 12 h; after that, it

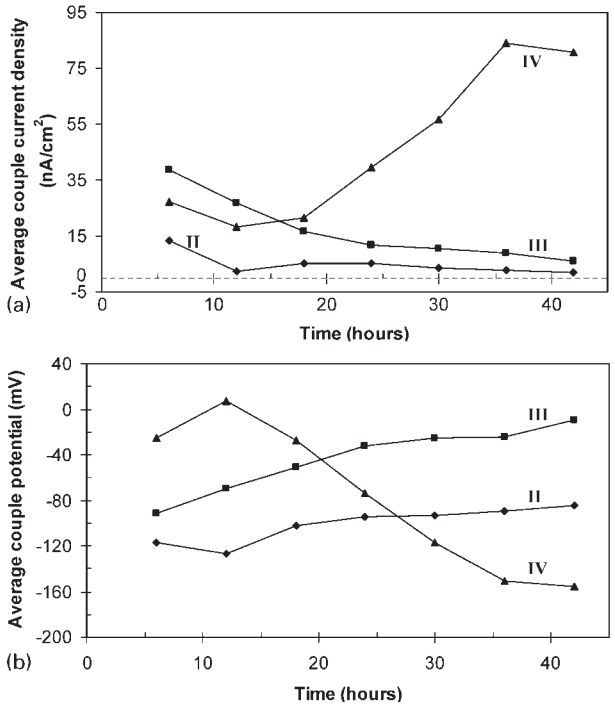

10 ***a*** **average galvanic couple current density and** ***b*** **average couple potential of weld–base galvanic couples in II, III and IV during 42 h exposure time in 3·5%NaCl solution. Average values of data for 10 min measurements were used**

increases rapidly up to more than 80 nA cm^{-2} to 42 h exposure time, reaching an almost steady state.

Considering the measured galvanic current of three couples (Fig. 10*a*), which reveals higher current density for IV, the amount of current measured depends on the existing thermodynamically cell driving force, and consequently, the extension of difference on microstructure of the anode and cathode parts. As mentioned before in the section on 'Microstructure evaluation', employing PWHT reduces the dissimilarity of microstructure in between base and weld regions and removes HAZ. Therefore, the cell driving force decreases, which is more enhanced in II and III. Interestingly, while the driving force (OCP difference) for base–weld couple in IV is less than that in III; after 12 h, this value begins to increase and becomes bigger than the one in III, reaching the maximum value after 42 h. Apparently, aging heat treatment at 620°C (IV) shows no significant improvement in reducing galvanic corrosion current compared to as weld specimen.[16] This is an indication of existence of distinguished microstructure difference between base and weld regions in IV, which can be attributed to volume fraction of ferrite, morphology and distribution of copper rich precipitates and the amount of reverted austenite.

Concerning the influence of reverted austenite, it has been reported that copper precipitates are expected to be a favourable nucleation site for reversed austenite, since both copper and austenite have the same face centred cubic (fcc) structure with the similar lattice parameter. During aging at high temperature above 600°C, segregation and diffusion of austenite stabiliser's Cu, Ni and Fe atoms would have a profound influence on the precipitates and the martensite matrix and lead to austenite forming element enriched areas around the copper precipitates, which could trigger reversed austenite to nucleate. Cr content, which is ferrite former, conversely decreases in the reverted austenite. Therefore, C and N, which are also austenite stabilisers, may be concentrated to the reverted austenite.[2,21] Furthermore, the growth of reversed austenite attracted considerable amounts of Cu and Ni from the martensite matrix, since the solubility of these elements in austenite is much higher.[2,5,21] The reverted austenite is a stable phase only in the IV condition, which encompassed the ε-copper rich precipitates. This phenomenon has not been reported in II and III.[2] Overall effects of the above parameters are expected to be the reason that higher galvanic current was monitored in IV compared to II and III. In addition, the presence of white lamellar recrystallised alpha ferrite (Fig. 5), which has the highest value in IV (both in size and volume fraction), could also be another reason that helps to explain different currents observed in II, III and IV. This phase does not exist in II. In II, during precipitation of copper, coherent body centred cubic (bcc) clusters nucleate, and by increasing the aging temperature in III, they grow in the supersaturated bcc matrix, lose slightly their coherency, and then by further increasing aging in IV, they subsequently transform to incoherent fcc ε-copper rich precipitates, reaching to a certain critical size around 30 nm.[2,19] Therefore, coarsening and lower coherency of precipitates in higher aging temperature results in more galvanic current in IV. More investigations with accurate techniques, such as TEM, are needed to determine the microstructure influence and corrosion initiation sites and elucidate the exact mechanism.

Galvanic couple potential in Fig. 10*b*, reveals an increase in couple potential in II and III (with more enhanced) from −117 and −90 mV to −85 and −10 mV respectively. Increasing couple potential and simultaneously decreasing couple current is an indication of anodic polarisation, which indicates the consistency and continuity of passivity on both electrodes, base and weld regions in II and III and more promoted in II. On the contrary, couple potential in IV is slightly increased in the beginning, and then after 12 h, it constantly decreases from 7 down to −155 mV. Decreasing in couple potential and simultaneously increasing in galvanic current density after 42 h immersion may be an indication of possible anodic depolarisation, here, base region rather than depolarisation of cathode. This observation shows clearly less integrity in passivity of anode, here base region, in IV compared with II and III. None of the couple potentials reached the stable state, which means that no equilibrium conditions can be achieved between the cathode and the anode of cell within 42 h. Concerning the high current measured in IV, it should be notice that, in reality, due to lower kinetic effect of anode/cathode surface area ratio (compared to experimental samples with identical cathode and anode surface area), the current may be smaller than this. Therefore, ZRA test result may overestimate the extension of galvanic corrosion occurrence in IV.

In summary, from a galvanic corrosion point of view and based on the results obtained by ZRA method, PWHT of GTA repair weldment in 17-4PH stainless steel in 3·5%NaCl solution improves the corrosion resistance. The galvanic current densities of a few to

tenths of nanoampere per square centimetre were detected. Aging at 620°C has the highest driving force for galvanic corrosion occurrence and the highest risk among the three heat treated sample. The results also reveal that HAZ has disappeared by solution annealing before aging.

Consider formation of a galvanic cell compromising a weld as cathode and base as the anode of all the cells. On the weld zone, the cathodic current reaction is more feasible (comparing the cathodic branch of weld and base regions in polarisation curve of II, III and IV, Fig. 7) predominantly belongs to oxygen reduction reaction current on weld surface constituents (cathodic current associated to the individual surface constituents is not clear). During galvanic coupling of weld to base, the anodic reaction of weld zone is very small and mainly attributed to the passivity current. On the other hand, in anode part, the base, the anodic current reaction is more feasible (comparing the anodic branch of base and weld regions in polarisation curve of II, III and IV, Fig. 7) and predominantly associated to the passivity current of the surface constituents. Although anodic polarisation of base may cause formation of pitting corrosion in the weakest phase in the long term, distinguishing the fraction of anodic current associated to passivity and pitting is not straightforward to obtain. Obviously, during galvanic coupling of base to weld region, a very small amount of oxygen reduction as cathodic reaction in base also occurred. In summary, the overall current measured by ZRA method is exactly the net current associated with the base as anode that flows towards the weld as cathode as shown in Fig. 10.

It should be finally pointed out that the galvanic currents measured in the range of few nanoampere per square centimetre after 42 h exposure in an aggressive solution of 3·5%NaCl by ZRA indicates a proper repair welding operation following appropriate PWHT, resulting in an excellent corrosion resistance in weldment of 17-4PH stainless steel. Post-weld heat treatment at 480 and 550°C similarly leads to optimal corrosion resistance; however, concerning hardness measurements, aging at 480°C causes embrittlement in alloy. Post-weld heat treatment in 620°C not only has the advantage of reduced hardness but also its influence on corrosion resistance is negligible; therefore, it is not recommended. This is contrary to the only available results obtained by Nowacki on SMAW and FCAW of 17-4PH in 50% HNO_3 solution, where the author showed aging temperature at 620°C ensured better corrosion resistance.[12] However, welding procedure, the investigated corrosion media and method differ from the present study.

The measured couple current is the average value on the whole sample surface area and may underestimate the galvanic current sustainable due to galvanic couple and is not the measure of local current generated by individual constituents. In other word, the actual current in microscopical level are much more than the values measured by ZRA for the same area, as it has been reported elsewhere by employing the local probe technique SRET.[22] Therefore, although the galvanic current measured here by ZRA was not considerably high, but by generation of such this current, formation of stable pit in base metal can be predicted after long term exposure in sample PWHT at 620°C.

Conclusion

The aim of this work was to study the influence of PWHTs on the galvanic corrosion occurrence between base and weld pair of repair welded 17-4PH stainless steel in 3·5%NaCl. The results can be summarised as follows.

1. The most profit of PWHT was to remove the HAZ, which acted as anode in as welded specimen. By the disappearance of this region, the most kinetically dangerous couple weld–HAZ is vanished in weldment.
2. Slow scan rate potentiodyanimc polarisation measurement revealed that all PWHTs, particularly aging at 550°C, improve the passivity of weld region by increasing the pitting potential. Comparing OCP values obtained indicates that, in all conditions, base and weld regions act as the anode and the cathode respectively.
3. One hour measurement of galvanic couple between equal surface area of base and weld zone through ZRA configuration revealed an average current densities of 18, 18 and 100 nA cm^{-2} and were measured for galvanic couples of specimens aged at 480, 550 and 620°C respectively.
4. Results obtained after 42 h ZRA measurement showed that PWHTs improve the galvanic corrosion resistance, and the current densities of a few to tenths of nanoampere per square centimetre were detected, which is negligible in short time. Aging at 620°C has the highest risk among the three PWHTs with the highest galvanic couple current about 80 nA cm^{-2} after 42 h immersion.
5. The existence of slightly distinguishable microstructure difference between base and weld regions, particularly in sample aged at 620°C, may be attributed to the several factors including volume fraction of ferrite, morphology and distribution of copper rich precipitates and the amount of reverted austenite.

Acknowledgement

The authors would like to appreciate the financial support from Ferdowsi University of Mashhad for providing laboratory facilities during the period that this research was conducted. The authors also would like to acknowledge Dr K. Ranjbar in Ahvaz University for assisting on SEM examination.

References

1. J. R. Davis: 'ASM specialty handbook stainless steel', 34; 1994, Materials Park, OH, ASM International.
2. C. N. Hsiao, C. S. Chiou and J. R. Yong: *Mater. Chem. Phys.*, 2002, **74**, 132–142.
3. J. Wang, H. Zou, C. Li, S.-Y. Qiu and B. L. Shen: *Mater. Charact.*, 2006, **57**, 274–280.
4. J. D. Bressan, D. P. Daros, A. Sokolowski, R. A. Mesquita and C. A. Barbosa: *J. Mater. Process. Technol.*, 2008, **205**, 353–359.
5. J. H. Wu and C. K. Lin: *J. Mater. Sci.*, 2003, **38**, 965–971.
6. M. Murayama, Y. Katayama and K. Hono: *Metall. Mater. Trans. A*, 1999, **30A**, 345–353.
7. W. C. Chiang, C. C. Pu, B. L. Yu and J. K. Wu: *Mater. Lett.*, 2003, **57**, 2485–2488.
8. AK steel: '17-4PH stainless steel product data bulletin'; 2000, Middleton, OH, AK Steel Corp.
9. A. U. Malik, N. A. Siddiqi and I. N. Andijani: *Desalination*, 1994, **97**, 189–197.
10. K. Ferjutz and J. R. Davis: in 'ASM handbook', 10th edn, Vol. 6, 'Welding, brazing, and soldering', 482–490; 1993, Materials park, OH, ASM International.

11. J. C. Lippold and D. J. Kotecki: 'Welding metallurgy and weldability of stainless steel', 264–286; 2005, New York, NY, Wiley.
12. J. Nowacki: *J. Mater. Process. Technol.*, 2004, **157–158**, 578–583.
13. M. P. Satish Kumar and P. Bala Srinivasan: *Mater. Lett.*, 2008, **62**, 2887–2890.
14. C. Garcia, F. Martin, P. de Tiedra, Y. Blanco and M. Lopez: *Corros. Sci.*, 2008, **50**, 1184–1194.
15. C. T. Kwok, S. L. Fong, F. T. Cheng and H. C. Man: *J. Mater. Process. Technol.*, 2006, **176**, 168–178.
16. M. R. Tavakoli Shoushtari, M. H. Moayed and A. Davoodi: *Corros. Eng. Sci. Techol*, 2011, **46**, 409–417.
17. 'Standard specification for age-hardening stainless steel forgings', ASTM A 705, Annual Book of ASTM Standards, Philadelphia, PA, USA, 1996.
18. L. W. Tsay, W. C. Lee, R. K. Shiue and J. K. Wu: *Corros. Sci.*, 2002, **44**, 2101–2118.
19. H. R. Habibi Bajguirani: *Mater. Sci. Eng. A*, 2002, **A338**, 142–159.
20. P. Ernst, N. J. Laycock, M. H. Moayed and R. C. Newman: *Corros. Sci.*, 1997, **39**, 1133–1136.
21. H. Nakagawa, T. Miyazaki and H. Yokata: *J. Mater Sci.*, 2002, **35**, 2245–2253.
22. R. Akid and D. J Mills: *Corros. Sci.*, 2001, **43**, 1203–1216.